

Human Serum Albumin-Inspired Glycopeptide-Based Multifunctional Inhibitor of Amyloid- β Toxicity

Rajsekhar Roy, Krishnangsu Pradhan, Juhee Khan, Gaurav Das, Nabanita Mukherjee, Durba Das, and Surajit Ghosh*

Cite This: *ACS Omega* 2020, 5, 18628–18641

Read Online

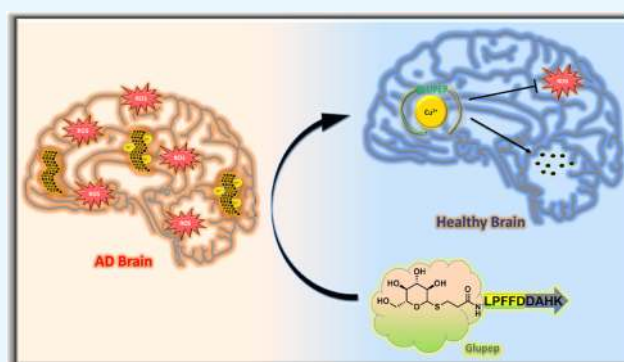
ACCESS |

Metrics & More

Article Recommendations

Supporting Information

ABSTRACT: In Alzheimer's disease (AD), insoluble A β 42 peptide fragments self-aggregate and form oligomers and fibrils in the brain, causing neurotoxicity. Further, the presence of redox-active metal ions such as Cu²⁺ enhances the aggregation process through chelation with these A β 42 aggregates as well as generation of A β 42-mediated reactive oxygen species (ROS). Herein, we have adopted a bioinspired strategy to design and develop a multifunctional glycopeptide hybrid molecule (Glupep), which can serve as a potential AD therapeutic. This molecule consists of a natural metal-chelating tetrapeptide motif of human serum albumin (HSA), a β -sheet breaker peptide, and a sugar moiety for better bioavailability. We performed different biophysical and docking experiments, which revealed that Glupep not only associates with A β 42 but also prevents its self-aggregation to form toxic oligomers and fibrils. Moreover, Glupep was also shown to sequester out Cu²⁺ from the A β -Cu²⁺ complex, reducing the ROS formation and toxicity. Besides, this study also revealed that Glupep could protect PC12-derived neurons from A β -Cu²⁺-mediated toxicity by reducing intracellular ROS generation and stabilizing the mitochondrial membrane potential. All these exciting features show Glupep to be a potent inhibitor of A β 42-mediated multifaceted toxicity and a prospective therapeutic lead for AD.



1. INTRODUCTION

Alzheimer's disease (AD), the most common and severe form of dementia, has remained elusive and needs further understanding at the molecular level. The most common symptoms of this disease are cognitive loss, dementia, behavioral discrepancy, etc.¹ The multidirectional nature of AD makes it extremely challenging to achieve effective therapy for this devastating disease.² Major advancements in disease progression through molecular-level understanding in the last decade have established several hypotheses related to AD such as (i) the cholinergic hypothesis,^{3–5} (ii) amyloid hypothesis,⁶ (iii) metal ion hypothesis,⁷ (iv) Tau hypothesis,⁸ (v) oxidative stress,⁹ etc. Among these, generation of senile plaques from deposits of amyloid- β (A β) has always been suspected of playing a significant role in disease progression. Moreover, it is also suspected of having a mutual relationship with all other pathological hypotheses.⁴

The A β peptide (40–42 amino acid-long amphiphilic peptide) undergoes a self-assembling process and forms oligomeric aggregates followed by fibrillar aggregates.¹⁰ These aggregates are mainly considered to be the cause of A β -mediated toxicity.¹¹ Therefore, the development of a chemical modulator that can prevent the aggregation of the A β peptide had been a significant focus for AD treatment.¹²

Recent literature reports reveal many peptide-based molecules that have been designed and explored based on their inhibitory role in A β aggregation. Tjernberg et al. demonstrated that the KLVFF short peptide, the 16–20 residues of the A β hydrophobic core, inhibits the aggregation of A β .¹³ Rajsekhar et al. showed that peptide residues KLVFF from the A β hydrophobic core can act as a recognition moiety and can be modified to develop multifunctional therapeutics against AD.¹⁴ Lowe et al. showcased that attaching a lysine hexamer to the recognition moiety as a disrupting element decreases A β -mediated toxicity.¹⁵ Soto et al. modified the recognition moiety KLVFFA and constituted a pentapeptide (LPFFD) that has antifibrillary activity.¹⁶

The brain strictly scrutinizes the transport of biomaterials (such as Cu²⁺, Zn²⁺, Fe²⁺, Ca²⁺) required for its normal functioning.¹⁷ It has been documented before that disbalance in neuronal homeostasis of these metal ions may play a crucial

Received: March 6, 2020

Accepted: May 19, 2020

Published: July 20, 2020



role in AD pathogenesis.¹⁸ Moreover, the metal ion hypothesis has always linked the presence of redox-active bio-metals to the generation of reactive oxygen species (ROS) that induce A β toxicity.¹⁹ Although initially A β was believed to produce ROS voluntarily,²⁰ later on, it was reported that the presence of metals is necessary for the production of ROS in the AD brain.²¹ Among all the metals, copper has always been found in amyloid plaques at high concentrations (~ 0.4 mM), which accelerates amyloid aggregation.²² At the oxidized state, Cu²⁺ binds to A β , receives an electron from methionine (Met-35), and gets reduced to the A β -Cu⁺ state, which is catalyzed by biological reductants like ascorbate.²³ Due to its excessive metabolic needs, the brain consumes 20% of the total oxygen of the body. Therefore, the brain is considered to be the most oxygen abundant organ compared to any other organs in the body.²⁴ A β -Cu⁺ takes part in an uncontrolled redox reaction and reduces these abundant molecular oxygens, eventuating H₂O₂.²⁵ This H₂O₂, later on, participates in a Fenton-type reaction with A β -Cu⁺ and generates hydroxyl radicals (\cdot OH), in turn causing oxidative stress and finally neuronal death in the AD brain.²⁶ Many metal ion chelators have been developed and also been reported to reduce A β -Cu²⁺-mediated ROS production and its toxicity. Clioquinol (CQ) and 8-hydroxyquinoline (PBT2) have been shown to chelate copper and to cause improvement against ROS-mediated toxicity.²⁷ Qu et al. adopted the same fashion and cast CQ on nanoparticles, which showed a successful reduction of ROS-mediated toxicity in the AD brain.²⁸ Although ROS-mediated toxicity was reduced through chelating copper, extracellularly assembled A β peptides aggregate to form toxic oligomers and finally developed into fibrils.

As a whole, multifactorial toxicity induced by A β with or without the involvement of metals leads to neuronal damage and disease advancement. Although different approaches have been used against the A β -mediated toxicity (either a β -sheet breaker or metal chelator), all these approaches alone have failed to work satisfactorily in AD treatment. Therefore, developing a multifunctional chemical component that can inhibit A β aggregation along with its ROS-mediated toxicity through metal sequestration from the A β -Cu²⁺ complex would be a highly favorable approach. In this context, various bifunctional peptide molecules have been designed and investigated according to their ability to disaggregate A β and their ability to interfere with metal-mediated ROS generation. Faller et al. discovered A β 12–20 and 13–20 residues to have an inhibitory aggregation effect along with a metal chelating ability.²⁹ Yuan et al. followed a similar way and formulated bifunctional peptide GGHRYYA AFFARR (GR), where the sequence GGH is used for metal chelation and the rest of the sequence was used to create an inhibitory aggregation effect.³⁰ Recently, Rajasekhar et al. interestingly modified the recognition moiety KLVFF using sarcosine and attached a natural copper-chelating sequence GHK to form SrVSrFSrGHK (P6), which showed both aggregation-inhibiting and metal-chelating properties.³¹ The human body contains several naturally occurring metal chelating peptide motifs known as the amino terminal Cu²⁺- and Ni²⁺-binding motif (ATCUN).³² Biologically available proteins or peptides containing these motifs have specific selectivity and high affinity toward the metal ions. Only a small number of studies have shown whether these motifs can be utilized as peptide metal chelators. In this context, Asp-Ala-His-Lys (DAHK), a natural tetrapeptide ATCUN derived from human serum

albumin (HSA), can be modified to constitute a multidirectional inhibitor for A β toxicity. A chemically synthesized DAHK motif of HSA binds to Cu²⁺ predominantly in a 1:1 stoichiometry with binding affinity of $K_a \sim 10^{14}$ for Cu²⁺, which is much higher than of A β 's Cu²⁺ binding affinity of $K_a \sim 10^9$.³³ Upon chelating to DAHK, Cu²⁺ gets bound into a square planar geometry. This type of structure hinders the reduction of Cu²⁺ to Cu⁺ as Cu⁺ prefers a tetrahedral geometry. The inhibition of this reduction, in turn, terminates the whole redox cycle.^{34–36} Although it is the most abundant protein in blood serum (concentration of ~ 640 μ M), HSA is present in a relatively smaller amount (3 M) in cerebrospinal fluid (CSF).³⁷ This can be correlated with increased ROS-mediated toxicity in the AD brain as the smaller abundance of HSA in CSF limits the presence of DAHK in the brain. To counter this, chemically synthesized DAHK containing a peptide-mimicking inhibitor of multifaceted A β toxicity has been conceptualized in this article. Moreover, to justify its relevance, it has been reported that synthesized DAHK alone can reduce copper-mediated ROS induction and neuronal toxicity.³²

In this study, DAHK has been thoughtfully coupled with the A β 42 recognition moiety, LPFFD, which on its own has an A β aggregation inhibitory effect. As a whole, this newly synthesized molecule is expected to show multidirectional activity through A β aggregation inhibition and reduction of ROS-generated toxicity through copper chelation. Besides, due to its much higher binding affinity, it is also expected to chelate out copper from the A β -Cu²⁺ complex. Despite being designed to be a potent inhibitor of A β aggregation and ROS generation, this molecule is not equipped to overcome the concern regarding the peptide's instability in biological conditions. The peptide's susceptibility to serum proteases has been a major obstacle in its use as a synthesized therapeutic component.³⁸ In recent studies, several strategies such as N-substitution, cyclization, incorporation of sarcosine, turn mimetics, and glycoconjugation have shown to increase the peptide's stability in biological conditions.³⁹ Among these, glycoconjugation has shown an additional propensity to increase the A β disaggregation by peptide molecules.⁴⁰ Sinopoli et al. showed in their work that attaching a monosaccharide trehalose molecule to recognition moiety LPFFD not only enhanced its serum stability but also showed an increased disaggregation of A β aggregates.⁴¹ It has also been speculated that just covalently attaching a monosaccharide unit to a short-sequence peptide can introduce steric hindrance and thus help the peptide participate in disaggregation.⁴² On this basis, the designed nonapeptide sequence (LPFFDDAHK) is modified by conjugating a glucose molecule through thio-coupling, thus constructing the glycopeptide, Glupep. The glycocomponent upon getting coupled to a peptide is anticipated to enhance the peptide's stability against serum proteases and also augments its aggregation disruption ability. Different techniques such as the thioflavin-T (ThT) assay and dot blot analysis were carried out to determine the A β aggregation inhibitory ability of Glupep (Figure 9). The metal sequestration ability of Glupep (from the A β -Cu²⁺ inclusion complex) was evaluated in vitro using the tyrosine quenching assay. Later on, several in vitro studies have been performed to investigate the antioxidant property of Glupep. To examine the stability and bioavailability of the Glupep conjugate, a serum stability assay was performed. The therapeutic possibility of Glupep was then validated in vitro in PC12-derived neurons.

Overall, the studies reveal that structurally tuned, multifunctional Glupez effectively altered vital aspects of toxicity caused by $A\beta$ in AD.

2. RESULTS AND DISCUSSION

2.1. Design Strategy. As discussed earlier, here, we have adopted a bioinspired strategy to design Glupez from human serum albumin (HSA). Its copper-chelating motif (DAHK) has been coupled with a β -sheet breaker peptide (LPFFD), to stop the generation of reactive oxygen species (ROS),⁴³ and a glucose moiety has been coupled with the N-terminal of the nonapeptide to enhance its serum stability, bioavailability, and membrane permeability (Figure 1).⁴⁴ This glycopeptide

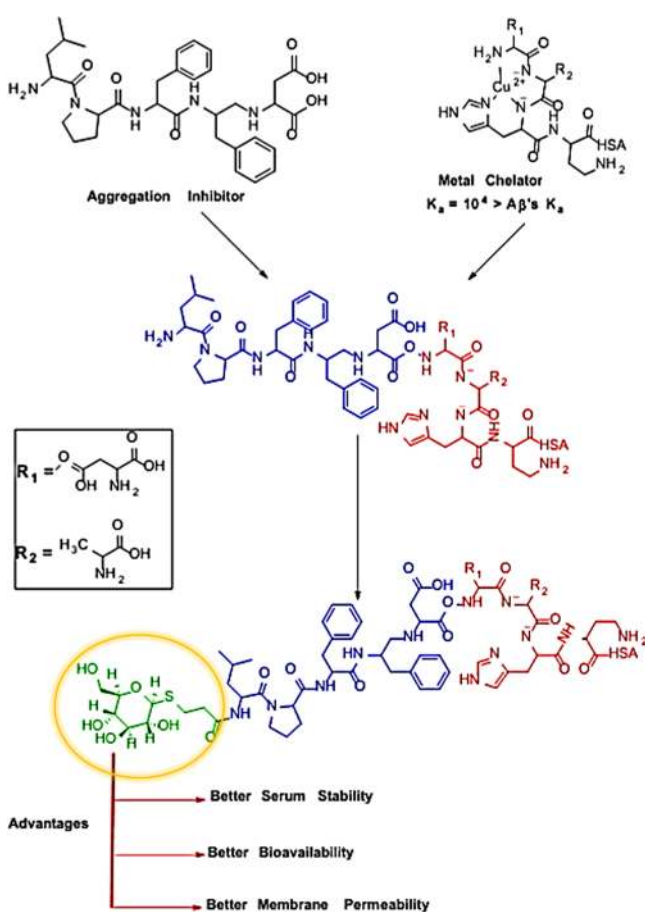


Figure 1. Schematic representation of the design concept of glycopeptide "Glupez".

(Glupez) is expected to inhibit the redox cycle by extracting Cu²⁺ from the A β 42–Cu²⁺ complex and impede Cu²⁺-dependent and Cu²⁺-independent aggregation of A β 42.

2.2. ThT Assay to Explore the Inhibitory Effect on A β 42 Fibrillation. A β 42 fibrils play a crucial role in disease progression in the AD brain. Therefore, inhibiting the formation of these aggregates is regarded as one of the most crucial strategies for designing effective therapeutics for AD. The thioflavin-T (ThT) assay was performed to understand the effect of Glupez on A β fibrillation. ThT ($\lambda_{\text{ex}} = 445$ nm, $\lambda_{\text{em}} = 485$ nm), a benzothiazole-based fluorescent dye, shows minimum fluorescence in the presence of A β 42 monomers, but an increment in fluorescence occurs when it interacts with mature A β aggregates.⁴⁵ Therefore, the change in fluorescence

intensity of ThT can be considered as a marker for A β fibrillation alteration. For this study, A β 42 (10 μ M) was incubated alone (control) and co-incubated separately in the presence of different concentrations of Glupez (2.5–20 μ M) at 37 $^{\circ}$ C with constant agitation for 48 h. Then, the fluorescence intensity of the ThT was measured at 485 nm to estimate the effect of increasing concentration on fibrillation. From the ThT fluorescence intensity, it is prominent that with an increment in the concentration, inhibition of fibrillation also improved (Figure 2A). Thus, this implies Glupez to have a dose-dependent inhibitory effect on A β 42 fibrillation. Further, Glupez (10 μ M), LPFFD (10 μ M), DAHK (10 μ M), and glucose (10 μ M) were co-incubated with a fixed concentration of A β 42 (10 μ M) to estimate the effect of increasing concentration on fibrillation. From the results (Figure 2C), it is prominent that glucose and DAHK have the least significant effect on A β 42 fibrillation. LPFFD (positive control) showed a 32% decrease of fluorescence intensity, indicating an effective inhibition. Surprisingly, Glupez showed a 63% reduction in the ThT fluorescence intensity, reflecting the significant inhibitory effect on A β 42 fibrillation, which is 30% greater inhibition than that of the positive control with an increment in the concentration, and inhibition of fibrillation also improved.

2.3. Dot Blot Assay to Determine the Effect on A β 42 Fibrillation. Preliminary studies with ThT showed Glupez to be an effective dose-dependent inhibitor of A β 42 fibril aggregation. The dot blot assay was performed to confirm this result.⁴⁶ A β 42 (10 μ M) along with different amounts of Glupez (2.5–20 μ M) were co-incubated separately to form fibrillar aggregates. These samples were then spotted on a nitrocellulose membrane and then subjected to treatment with the OC antibody (detects fibrillar aggregates only). The control samples were treated with the 6E10 antibody (detects all forms of A β 42). After measuring the intensities of the spots, Glupez showed a concentration-dependent inhibition toward A β 42 fibril formation. Concentrations of 5, 10, and 20 μ M showed inhibition of 10, 73, and 91%, respectively (Figure 2B). This data supports the result of the ThT assay and confirms that Glupez effectively inhibits A β 42 aggregation to form fibrils and hence aggregation (Figure S5).

2.4. ThT Assay to Investigate the Inhibitory Effect on A β 42 Oligomer Formation. Oligomers are believed to be the most toxic form among all the polymorphic forms of the A β 42 peptide, which precipitate at synaptic junctions and cause neurotoxicity by disrupting synaptic plasticity.^{47,48} Many of the aggregation inhibitors reported in the literature are known to arrest the aggregation process at an oligomeric state only; hence, they do not properly inhibit the toxicity.⁴⁹ In this experiment, Glupez was studied for its oligomerization inhibitory effect using the ThT assay. The A β 42 peptide (10 μ M) was incubated alone and with DAHK (10 μ M), LPFFD (10 μ M), and glucose (10 μ M), individually at 37 $^{\circ}$ C for 1 h and then for 24 h at 4 $^{\circ}$ C. The fluorescent dye thioflavin-T (ThT) was used to detect the remaining A β 42 oligomers ($\lambda_{\text{ex}} = 445$ nm, $\lambda_{\text{em}} = 485$ nm). The result (Figure 2F) showed that glucose is the least effective against oligomerization. DAHK was shown to decrease the intensity by 45%. A solution co-incubated with LPFFD (positive control) prohibited oligomer formation by 57% compared to the control (A β 42 only). Surprisingly, Glupez showed the largest effectivity and, as a result, showed that 91% of the oligomers disaggregated after incubation. Next, the same experiment was repeated using

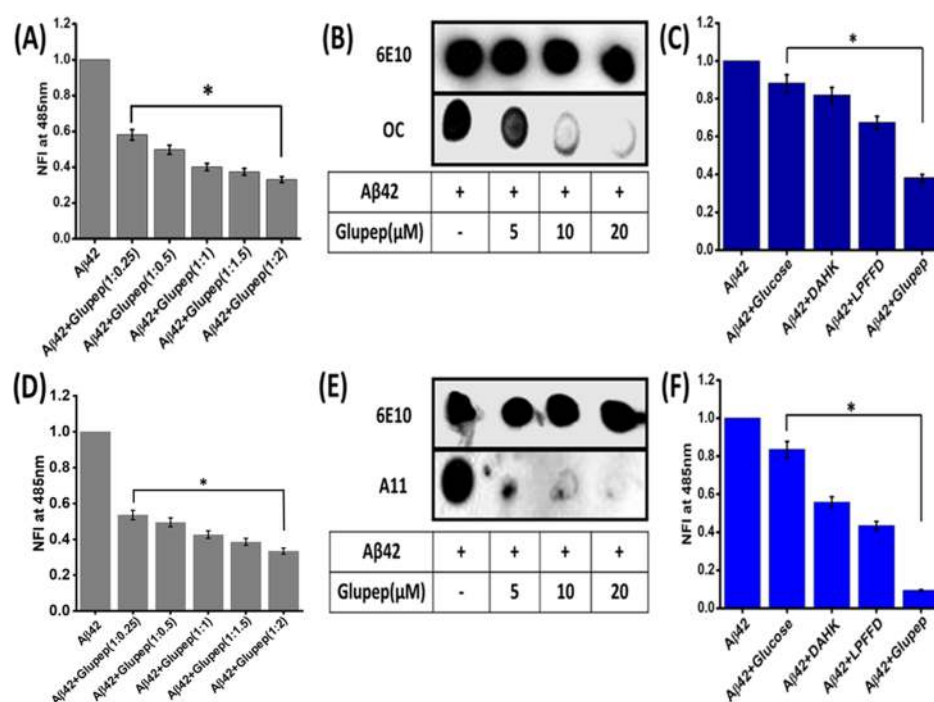


Figure 2. (A) Inhibition of amyloid fibrillation detected through the ThT assay in the presence of GluPeP in different concentrations. (B) Assessment of inhibition of amyloid fibrillation using the dot blot assay. (C) Bar diagram of the ThT assay to detect the inhibition of components (Glucose, LPFFD, and DAHK). (D) ThT assay of amyloid oligomer inhibition in the presence of GluPeP in different increasing concentrations. (E) Dot blot assay to detect inhibition of amyloid oligomerization in increasing GluPeP concentrations. (F) Histogram of the ThT assay with various components (glucose, LPFFD, and DAHK) for amyloid oligomer inhibition. Error bar corresponds to the standard deviation of the value ($*p \leq 0.05$) of the normalized fluorescence intensity (NFI).

increasing concentrations of GluPeP (2.5–20 μM). Solutions incubated with a higher concentration of GluPeP exhibited higher efficacy than those with lower concentrations (Figure 2D), ensuring the concentration-dependent inhibitory effect of GluPeP on Aβ42 oligomerization.

2.5. Detecting Inhibition of Aβ42 Oligomerization by the Dot Blot Assay.⁵⁰ Following the ThT assay, the dot blot assay was performed to confirm GluPeP's ability to inhibit oligomer formation. For this, Aβ42 (10 μM) was incubated alone and also with varying concentrations of GluPeP (5, 10, and 20 μM) in PBS (10 mM, pH = 7.4) to generate the oligomers. Each sample (2 μL) was then spotted on a nitrocellulose membrane in two sets. One set was incubated with A11 antibodies, which can detect oligomers only, and the other set (control) was incubated with 6E10, which detects any form of the Aβ42 peptide. Comparing the intensities between the two sets showed a concentration-dependent inhibitory effect of GluPeP against Aβ42 oligomerization (Figure 2E). Plotting the intensity against concentration (Figure S6) showed that unlike most of the reported aggregation inhibitors, GluPeP not only inhibits the generation of more Aβ42 aggregates but also disrupts the formation of Aβ42 oligomers.

2.6. Effect of GluPeP on Cu²⁺-Mediated Aβ42 Aggregation. Previously, several studies have suggested that even a minimal amount of Cu²⁺ (Aβ42: Cu²⁺ = 1:0.4) can chelate and accelerate Aβ42 aggregation.⁵¹ Therefore, to function as an Aβ42 aggregation inhibitor, GluPeP should also have an inhibitory effect on Cu²⁺-mediated Aβ42 aggregation. To assess the inhibitory effect of GluPeP, Aβ42 (10 μM) was co-incubated with Cu²⁺ (4 μM) as a control solution, and then the control solution was separately co-incubated with DAHK (10 μM), LPFFD (10 μM), glucose (10

μM), and GluPeP (10 μM). Lastly, ThT (10 μM) was used to detect and quantify aggregation inhibition. The result showed that glucose has the least effect on aggregation. DAHK (copper chelator) was shown to reduce the aggregation by 32%. Positive control LPFFD was shown to inhibit the fluorescence intensity by 42%. Meanwhile, designed inhibitor GluPeP showed 69% reduction in the intensity (Figure S7). The result has confirmed the exceptional inhibitory effect of GluPeP on copper (Cu²⁺)-mediated Aβ42 aggregation.

2.7. Understanding the Molecular Interactions of GluPeP with Aβ42 Aggregates. Previous experiments have demonstrated the inhibitory activity of GluPeP against Aβ42 oligomerization and fibril aggregation. Molecular docking studies were carried out with the corresponding Aβ42 monomer (PDB ID: 1IYT)⁵² and Aβ42 fibril (PDB ID: SKK3)⁵³ for a detailed understanding of the mechanism of inhibition. Docking studies revealed that GluPeP binds to the ⁶HDSGYEVHHQKLVFFA²¹ region containing the hydrophobic core ¹⁶KLVFFA²¹ of the Aβ42 peptide monomer with a binding energy of −5.2 kcal/mol through polar interactions (Figure 3A–D). ASP7, SER8, GLU11, VAL12, LYS16, and ASP23 amino acids were the prominent residues interacting with GluPeP. Docking studies performed for the monomer with glucose, LPFFD, and DAHK showed interaction energies of −4.4, −3.8, and −4.7 kcal/mol, respectively (Figures S16–S18). Docking studies performed with the Aβ42 fibril established the interaction of GluPeP with GLU11, HIS13, HIS14, VAL40, and ILE41 residues (BE of −7.2 kcal/mol) (Figure 3E,F). In contrast to GluPeP, DAHK, LPFFD, and glucose were shown to interact with the fibril with binding energies of −5.7, −5.9, and −4.8 kcal/mol, respectively (Figures S8–S10), which are insignificant compared to that

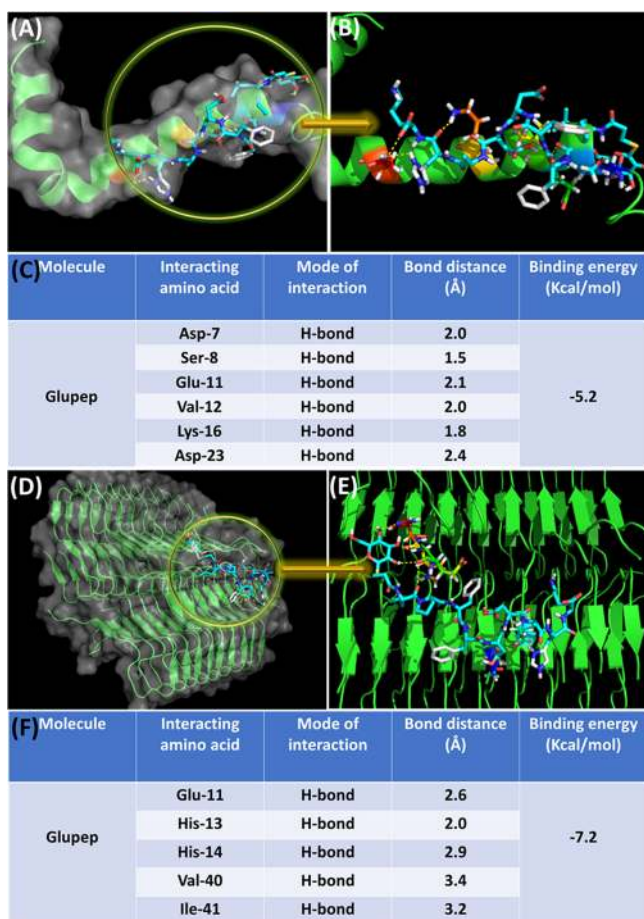


Figure 3. (A) Molecular docking experiment of Glupez with the A β 42 peptide monomer (PDB ID: 1IYT). (B) Bonding interaction of Glupez with the A β 42 monomer. (C) Summary of interacting amino acids and molecular interactions of Glupez with the A β monomer. (D) Molecular docking study of Glupez with the A β fibrillar aggregate (PDB ID: 5KK3). (E) Bonding interaction of Glupez with the A β 42 fibrillar aggregate. (F) Summary of interacting amino acids and molecular interactions of Glupez with the A β fibrillar aggregate.

of Glupez. Moreover, this study revealed Glupez to have an additional interaction between the hydroxyl group of the attached glucose with the aspartic acid residue of the A β 42 monomer and the histidine residue of the fibril. Interestingly, this interaction was missing in the case of LPFFD (positive control for aggregation inhibition). Altogether, the results of the study completely support the outcomes of ThT assays and Dot blot assays.

2.8. Analyzing the Copper Chelation Ability of Glupez. DAHK, the N-terminal ATCUN motif of HSA, was thoughtfully used in Glupez as a copper chelator, but the amide linkage between the two aspartic acid moieties concealed the N-terminal nitrogen of DAHK. Hence, assessment of Cu²⁺ chelation by Glupez was performed to check whether it has retained a similar ability with DAHK or not. For this experiment, absorption of Glupez (100 μ M) alone in PBS buffer (pH = 7.4, 10 mM) was measured by UV–vis spectroscopy, which exhibited an absorption maxima at 210 nm. Upon addition of Cu²⁺ (100 μ M), a shoulder peak at 268 nm was formed (Figure S11A), indicating successful chelation of Cu²⁺. Further, to understand the binding ratio between Glupez and Cu²⁺, a constant amount of Glupez (100 μ M) was

subjected to titration with different concentrations of Cu²⁺ (40–200 μ M). The shoulder peak at 268 nm showed a hyperchromic shift with an increment in concentration. Saturation in this shift appeared after the concentration of Cu²⁺ crossed 100 μ M, demonstrating that Glupez forms a complex with Cu²⁺ in a 1:1 stoichiometric ratio (Figure S11B). This experiment additionally confirmed that Glupez retains a similar Cu²⁺ chelating ability to DAHK.

2.9. Sequestration of Copper from the A β 42–Cu²⁺ Complex. In the presence of bioreductants (ascorbate), A β 42-bound Cu²⁺ gets reduced to Cu⁺ and initiates a reduction cycle, ultimately generating ROS.⁵⁴ Hence, we were interested in checking whether Glupez can sequester out A β -bound copper or not. For this, the inherent fluorescence of TYR10 present in A β was used. Due to its position and close vicinity to three histidine residues (His6, His13, His14), the fluorescence emission intensity of TYR10 can be altered by metal coordination.⁵⁵ It was reported that the fluorescence emission gets quenched by Cu²⁺, indicating the conformational change of the A β 42 peptide.⁵⁶ Upon sequestration of this Cu²⁺, TYR10 is expected to get back its characteristic emission peak at 308 nm. The magnitude of regaining the fluorescence intensity indicates the extent of the sequestering ability.

A β (10 μ M) was incubated in PBS (10 mM, pH = 7.4), and fluorescence emission was recorded to understand the aptitude of copper chelation by Glupez (Figure 4A). Emission spectra showed the characteristic peak of TYR10 at 308 nm. Following this, Cu²⁺ (10 μ M) was added into the A β solution and co-incubated, keeping the ratio at 1:1. The emission spectra this time showed a rigorous decrement of intensity owing to the quenching of TYR10. Remarkably, the addition of Glupez (10 μ M) was shown to restore the emission fluorescence to 82%

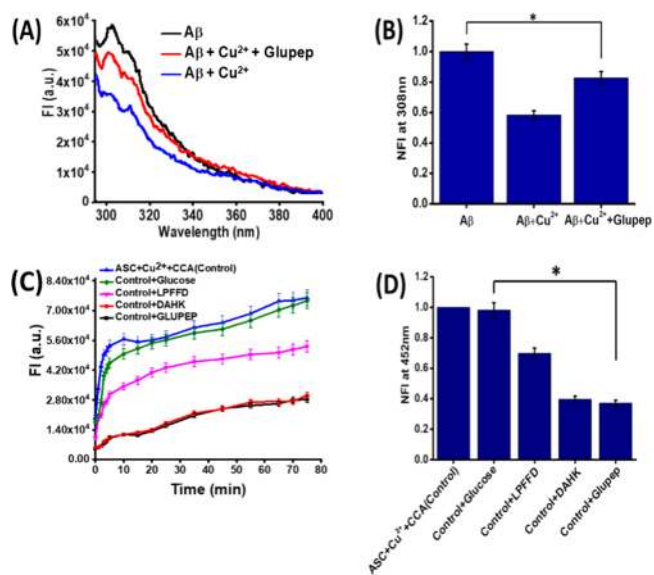


Figure 4. (A) Tyr10 fluorescence of only A β 42 (10 μ M) and A β 42–Cu²⁺ (1:1) (10 μ M) in the presence and in the absence of Glupez (10 μ M) in PBS buffer (10 mM, pH 7.4). (B) Bar diagram of Tyr10 normalized fluorescence intensity (NFI) measured for the A β 42–Cu²⁺ complex in the presence and absence of 10 μ M peptide Glupez. (C) Suppression of Cu²⁺-catalyzed ROS production through copper chelation via measuring the fluorescence intensity of 7-OH-CCA. (D) Bar diagram of corresponding fluorescence intensity of 7-OH-CCA at the end of 1 h. Error bar corresponds to the standard deviation of the value (* $p \leq 0.05$).

(Figure 4B). This signifies the ability of Glupez to chelate copper out of the $A\beta$ - Cu^{2+} complex, in turn preventing its redox cycle.

2.10. Suppression of Metal-Mediated ROS Generation by Glupez. In the AD brain, Cu^{2+} forms a complex with $A\beta_{42}$ and participates in the production of reactive oxygen species (ROS) through a Fenton-type reaction. Therefore, designing a proper antioxidant that can terminate the redox cycle of $A\beta$ - Cu^{2+} and sequentially prevent the ROS generation can be considered to be an appropriate approach to block the multifaceted toxicity in the AD. It has already been seen that Glupez can chelate and even sequester out $A\beta$ -bound Cu^{2+} . Thus, it is expected that Glupez is able to reduce $A\beta$ - Cu^{2+} -mediated ROS generation in the AD brain. Hence, to analyze whether Glupez is able to suppress redox formation or not, the ascorbate assay was performed. In this assay, Cu^{2+} was co-incubated with a natural reductant (ascorbate) to instigate the generation of hydroxy radicals, which is the most toxic form of ROS.⁵⁷ These hydroxy radicals convert nonfluorescent 3-coumarin carboxylic acid (3-CCA) to a fluorescence-active compound 7-hydroxy-coumarin-3-carboxylic acid (7-OH-3-CCA), which has a detectable fluorescence emission at 452 nm.

For this experiment, a solution having Cu^{2+} ($5 \mu M$), 3-CCA ($50 \mu M$), and deferoxamine ($1 \mu M$) was prepared in PBS (10 mM , $\text{pH} = 7.4$). Then, Glupez ($10 \mu M$), DAHK ($10 \mu M$), LPFFD ($10 \mu M$), and glucose ($10 \mu M$) were separately added to this solution. After the addition of ascorbate in a high amount ($150 \mu M$), these solutions were kept for incubation at 37°C for the next 70 min. Throughout this incubation period, fluorescence emission of formed 7-OH-3-CCA was recorded as a function of time at 452 nm ($\lambda_{\text{ex}} = 395 \text{ nm}$), keeping an interval of 5 min (Figure 4C). Glupez showed 63% reduction in generation of hydroxyl radicals at 70 min with respect to the control ($A\beta$ - Cu^{2+}), indicating that Glupez prevents the reduction process and forms a dormant redox complex with Cu^{2+} . On the other hand, comparing the result with that of positive control DAHK (61% reduction compared to control), Glupez showed a very similar outcome, indicating that the incorporation of DAHK into Glupez has no significant effects on its Cu^{2+} -chelating and ROS-inhibiting ability. Solutions containing LPFFD and glucose showed relatively higher fluorescence intensity, indicating their inability to reduce ROS generation. These outcomes (Figure 4D) suggested that even in a natural reducing environment, Glupez put a halt in the reduction process and in $A\beta$ - Cu^{2+} -mediated ROS generation.

2.11. Cell Viability Studies. Previous experiments performed in this study have suggested Glupez to be a multifunctional inhibitor of $A\beta_{42}$ aggregation and ROS generation. The next step is to perform in vitro studies to confirm its efficiency within cells. For this, the viable cellular concentration of Glupez must be determined by performing the MTT assay in rat pheochromocytoma (PC12) cells. Generally, the MTT assay determines the reduction potential of a live cell through colorimetric assessment. NADPH-dependent cellular enzyme oxidoreductase present in live cells reduces tetrazolium dye MTT (3-(4,5-dimethylthiazol-2-yl)-2,5-diphenyltetrazolium bromide) to form purple formazan.⁵⁸ Dead cells are incapable of carrying out this reduction process. Formazan produced in this reaction can be quantified by absorbance spectrometry (within 500–800 nm wavelength), indicating the percentage of viable cells present.

Herein, the PC12 cells were incubated in the presence of different increasing amounts (1.525 to $50 \mu M$) of Glupez at 37°C for 24 h, and then the MTT assay was performed. No cytotoxic effects were observed for Glupez at high concentrations of 50 and $100 \mu M$ (Figure S12), confirming Glupez to be safe for performing cell-based assays.

2.12. Restoring Cell Viability in the Presence of $A\beta$ - Cu^{2+} -Mediated Toxicity. In the AD brain, by forming a complex with $A\beta_{42}$, copper not only increases the extent of $A\beta_{42}$ aggregation but also induces ROS generation. In this context, to develop a multidirectional inhibitor, it must not only inhibit the aggregation and ROS generation but also should protect cells from toxicity. Hence, to determine the potential of Glupez, PC12 cells were treated with the $A\beta$ - Cu^{2+} complex ($10 \mu M$) and a high amount of natural reductant, ascorbate ($200 \mu M$), to induce toxicity. The cells were then incubated with different amounts of Glupez (1 – $20 \mu M$). The MTT assay was then performed to determine the percentage of rescued cells by Glupez (Figure 5A). $A\beta_{42}$ -

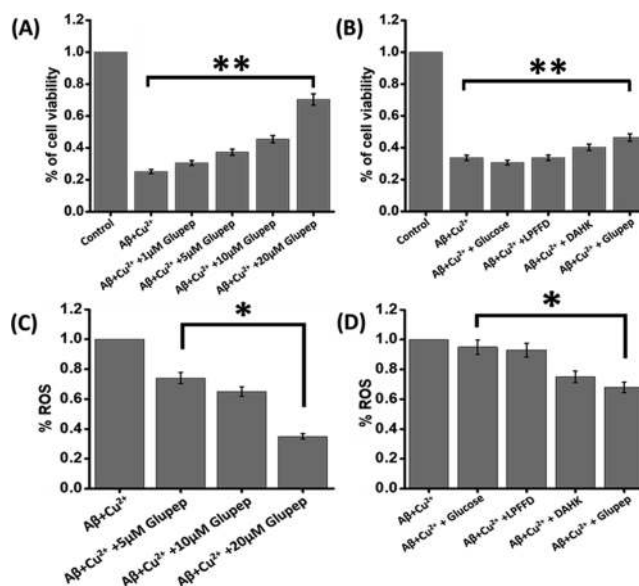


Figure 5. (A) Restoration of cell viability by Glupez in $A\beta_{42}$ - Cu^{2+} (1:1)-mediated toxicity (Cu^{2+} : $10 \mu M$), showing increased cell viability upon treatment with increasing concentrations of Glupez. (B) Comparing the ability to restore cell viability with glucose, LPFFD, DAHK, and Glupez in $A\beta_{42}$ - Cu^{2+} (1:1)-mediated toxicity showing increased cell viability upon treatment with increasing concentrations of Glupez. (C) Bar diagram for the DCFDA assay with increasing concentrations of Glupez. (D) Bar diagram for the DCFDA assay $10 \mu M$ glucose, LPFFD DAHK, and Glupez. Experiments were repeated in triplicate ($n = 3$), and the standard deviation (SD) was calculated, which is represented by the error bars. Error bar corresponds to the standard deviation of the value (* $p \leq 0.05$, ** $p \leq 0.03$).

Cu^{2+} -treated cells showed the highest toxicity with a cell viability of $\sim 25\%$ compared to untreated cells showing 100% viability. Meanwhile, the cell viability showed to increase 21% upon treating with Glupez at a concentration of $10 \mu M$. Doubling the concentration of Glupez to $20 \mu M$ showed enhancement in the cell viability to 70% (Figure 5A), thus suggesting the ability of Glupez to rescue the cells from $A\beta_{42}$ - Cu^{2+} -mediated toxicity in a dose-dependent manner. For a comparative assessment, a similar procedure was then

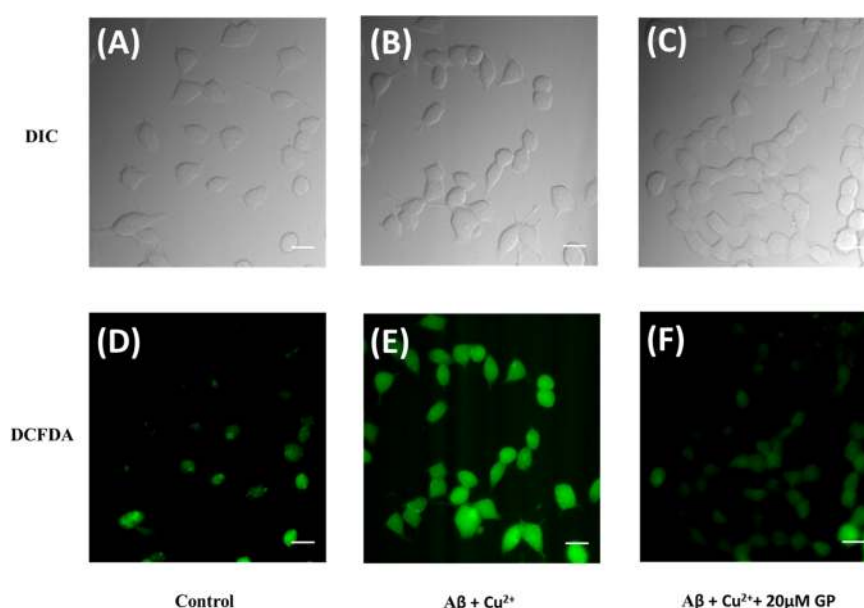


Figure 6. Live-cell microscopy images of PC12-derived neurons stained with DCFDA. DIC images of (A) untreated control PC12 cells, (B) $A\beta + Cu^{2+}$ -treated cells ($10 \mu M$) and (C) $A\beta + Cu^{2+}$ -treated cells ($10 \mu M$) in the presence of $20 \mu M$ GluPeP (GP). DCFDA images of (D) untreated control cells, (E) cells treated with $A\beta + Cu^{2+}$ ($10 \mu M$), and (F) cells treated with $A\beta + Cu^{2+}$ (1:2) in the presence of $20 \mu M$ GluPeP (GP). Scale bars corresponding to $20 \mu m$.

repeated with LPFFD ($10 \mu M$), DAHK ($10 \mu M$), and glucose ($10 \mu M$). Comparing the cell viability with that of $A\beta 42-Cu^{2+}$ -treated cells (Figure 5B) demonstrated LPFFD, DAHK, and glucose to either have no effect or a very negligible effect in restoring the cell viability.

2.13. In Vitro Assessment of ROS Suppression. As the primary in vitro analysis showed that GluPeP could protect cells from $A\beta 42-Cu^{2+}$ -induced toxicity, we were curious to know what kind of in vitro effect GluPeP will show on $A\beta-Cu^{2+}$ -mediated ROS generation. The effect of GluPeP on $A\beta 42-Cu^{2+}$ -induced ROS generation was studied using the DCFDA assay in PC12 cells.⁵⁹ DCFDA (2,7-dichlorofluorescein diacetate) is a nonfluorescent compound utilized to quantify ROS strains such as hydroxyl, peroxy, and other ROS species. DCFDA reacts with the ROS molecules formed from the $A\beta 42-Cu^{2+}$ -mediated redox cycle and gets oxidized to fluorescent 2,7-dichlorofluorescein (DCF, $\lambda_{ex} = 495 \text{ nm}$ and $\lambda_{em} = 529 \text{ nm}$). The PC12 cells were treated with DCFDA before incubating with $A\beta 42-Cu^{2+}$ ($10 \mu M$), a high amount of natural reductant ascorbate ($200 \mu M$), and amounts of GluPeP. Cells treated with increasing concentrations of GluPeP, that is, 5, 10, and $20 \mu M$, showed 25, 36.43, and 64.18% reduction in fluorescence intensity, respectively, compared to cells treated without GluPeP (Figure 5C), indicating the weaker presence of intracellular ROS with GluPeP treatment. This in vitro ROS suppression demonstrated by GluPeP can be correlated to its ability to sequester out copper from the $A\beta 42-Cu^{2+}$ complex. To compare this result with those of the component molecules, the assay was repeated with DAHK ($10 \mu M$), LPFFD ($10 \mu M$), and glucose ($10 \mu M$). Data (Figure 5D) revealed that LPFFD and glucose have no such antioxidant activity, and DAHK being the copper chelator reduced the fluorescence intensity by $\sim 25\%$ compared to control. Compared to the positive control (DAHK), GluPeP this time showed reduction in the intensity by almost $\sim 32\%$. To further confirm this in vitro antioxidant activity of GluPeP, we have performed imaging studies with DCFDA with

differentiated PC12 cells treated with the $A\beta 42-Cu^{2+}$ complex. As expected, $20 \mu M$ GluPeP showed reduction in the fluorescence intensity of DCFDA, as observed in $A\beta 42-Cu^{2+}$ complex-treated cells (Figure 6), and its DCFDA fluorescence intensity was more comparable to that of the untreated control PC12 cells (Figure S13), which is in agreement with the previous studies performed to elucidate the antioxidant potential of GluPeP. Hence, this result shows that the GluPeP molecule designed to terminate the $A\beta 42-Cu^{2+}$ -mediated redox cycle is confirmed to possess the desired characteristics, and also, the result is in good support of the outcome obtained from the ascorbate assay.

2.14. In Vitro Assessment of Mitochondrial Membrane Potential (MMP). $A\beta 42-Cu^{2+}$ leads to the induction of oxidative stress in neurons by the generation of ROS, which ultimately leads to mitochondrial dysfunction and depolarization of the mitochondrial membrane potential (MMP). Mitochondrial dysfunction is associated with the induction of cell death through activation of the apoptotic pathway. For assessing the mitochondrial membrane potential, the JC-1 assay has been performed through the quantitative analysis of the green/red intensity ratio. It was observed that $A\beta 42-Cu^{2+}$ at a $10 \mu M$ concentration leads to an abnormal increase in the green/red ratio in the PC12-derived neurons (Figure 7A,B), indicating that it induces MMP depolarization, which would ultimately result in mitochondrial dysfunction and cell death. However, in the presence of GluPeP at 20 and $10 \mu M$ concentrations, the green/red ratio of $A\beta 42-Cu^{2+}$ is severely reduced (Figure 7C,D) to the extent that it is comparable to the untreated control (Figure S14). Hence, we can conclude that GluPeP is a potent antioxidant molecule with the capability of reversing the various characteristics associated with the $A\beta 42-Cu^{2+}$ -mediated redox cycle.

2.15. Evaluation of Serum Stability. The above results suggest that GluPeP not only inhibits $A\beta 42$ aggregation but also has a similar ability to terminate ROS generation. However, a critical challenge for a peptide molecule to be

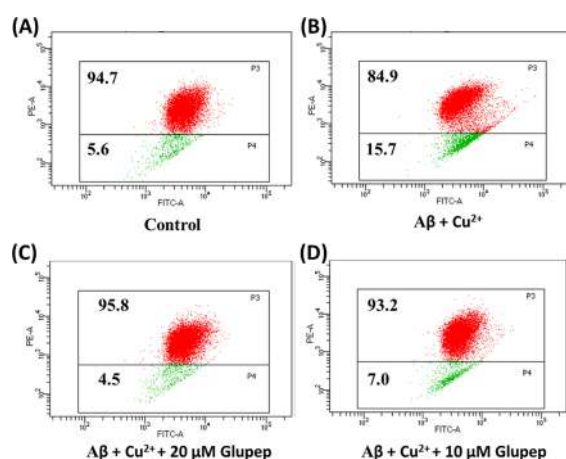


Figure 7. MMP assay with the JC1 dye of PC12-derived neurons (A) for untreated control PC12 cells, (B) after treatment with $10 \mu\text{M}$ $A\beta$ + Cu^{2+} , (C) when cells are co-incubated with $A\beta$ + Cu^{2+} and $20 \mu\text{M}$ Glu pep, and (D) when cells are co-incubated with $A\beta$ + Cu^{2+} and $10 \mu\text{M}$ Glu pep.

considered as a drug candidate is its susceptibility toward serum peptidases and lower bioavailability.⁶⁰ It has been described before that glycosylation of a peptide molecule has resulted in increased serum stability and enhanced bioavailability.⁶¹ Further, it also increases the peptide's side-chain protection from oxidation.⁶² Thus, we have attached the glucose moiety of our peptide at its N-terminal through thioconjugation to develop Glu pep.

To evaluate this strategy by determining the serum stability of the peptides (DAHK, LPFFD, LPFFDDAHK) and glycopeptide (Glu pep), molecules were incubated with 50% human blood serum for 24 h at 37°C and every 0, 4, 6, 12, and 24 h, the quantity of undamaged peptide was estimated using RP-HPLC (Figure 8A). Among all the molecules, DAHK was shown to have the least stability against serum proteases, with only 13% remaining intact after 24 h. LPFFD proved to be the second most susceptible peptide as only 32% of it remained undamaged after 24 h. LPFFDDAHK also showed to be unstable in serum as only 40% of it was intact after 24 h. Interestingly, attaching the glucose molecule with LPFFDDAHK and forming Glu pep has shown a positive impact on the stability as 84% of the Glu pep was still detected intact even after 24 h, that is, 44% more than the corresponding non-glycosylated analog LPFFDDAHK. This result suggested that the glycopeptide Glu pep has potential as a drug candidate for AD.

2.16. Inspecting Blood–Brain Barrier Permeability.^{58,59} Any molecule that is expected to have therapeutic relevance to Alzheimer's disease must possess the ability to cross the blood–brain barrier (BBB). For this reason, Glu pep was also inspected whether it has a BBB permeation ability or not. For this experiment, a 2.5 mM solution of Glu pep in saline was prepared, and a volume of $100 \mu\text{L}$ was injected intraperitoneally 6 h before the mice were sacrificed. After 6 h, the brain was isolated to prepare a homogenate in acetonitrile. Then, ESI-MS spectra revealed the presence of Glu pep molecular peaks, confirming Glu pep's ability to cross the BBB (Figure 8B). This experiment was repeated with the non-glycosylated counterpart of Glu pep, i.e., LPFFDDAHK. The ESI-MS spectra showed no molecular mass peak of

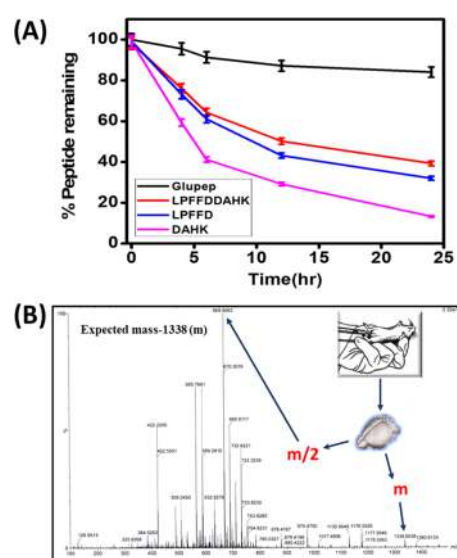


Figure 8. (A) Serum stability of Glu pep. Peptides (DAHK, LPFFD, LPFFDDAHK, and Glu pep) were incubated in human blood serum (HBS) and analyzed over a duration of 24 h. Each experiment was repeated three times ($n = 3$), and the standard deviation (SD) was calculated, which is represented by the error bars. Error bar represents the value of the SD ($*p \leq 0.03$). (B) ESI-MS mass spectra of mice brain homogenate treated with Glu pep. Expected mass (m): 1338 Da , observed mass: 669 Da [$m/2$], 1338 Da [m].

LPFFDDAHK (Figure S15), thus confirming that glycosylation has increased the BBB permeability of Glu pep.

3. CONCLUSIONS

In this paper, we showcased the design of a new glycopeptide-based inhibitor, which has the ability to target multiple vital issues of AD by targeting $A\beta_{42}$ aggregation and metal-induced ROS generation. The glycopeptide-based inhibitor was developed (Glu pep) by coupling a naturally occurring copper-chelating motif (DAHK) present in human serum albumin (HSA) with $A\beta_{42}$ aggregation inhibitory peptide LPFFD. We found that Glu pep inhibits both Cu^{2+} -dependent and Cu^{2+} -independent formation of $A\beta_{42}$ aggregates (oligomers and fibrils), and like native DAHK, Glu pep can also hamper the $A\beta_{42}$ – Cu^{2+} redox cycle by extracting out the Cu^{2+} , thus helping in maintaining a dormant redox state. We have also shown that Glu pep impedes ROS generation both in vitro and in vivo. It can also hold back depolarization of MMP in PC12-derived neurons induced by the $A\beta_{42}$ – Cu^{2+} redox cycle. Cell viability assay reveals that Glu pep not only protects the cells from $A\beta_{42}$ – Cu^{2+} -induced toxicity but also offers significantly better protection compared to its building components LPFFD and DAHK peptides. This study enabled us to overcome one of the significant concerns, serum susceptibility of therapeutic peptides, by attaching a glucose moiety to the N-terminal of Glu pep, which helps it cross the blood–brain barrier effectively. Considering all these aspects, we envision that this glycopeptide-based inhibitor Glu pep with its multifunctional inhibitory effects will contribute to designing efficient therapeutic leads against AD.

4. METHODS

4.1. Chemicals. All Fmoc protected amino acids and Rink amide resin was bought from Novabiochem (Germany). All the piperidines and 1,1,1,3,3,3-hexafluoroisopropanol (HFIP)

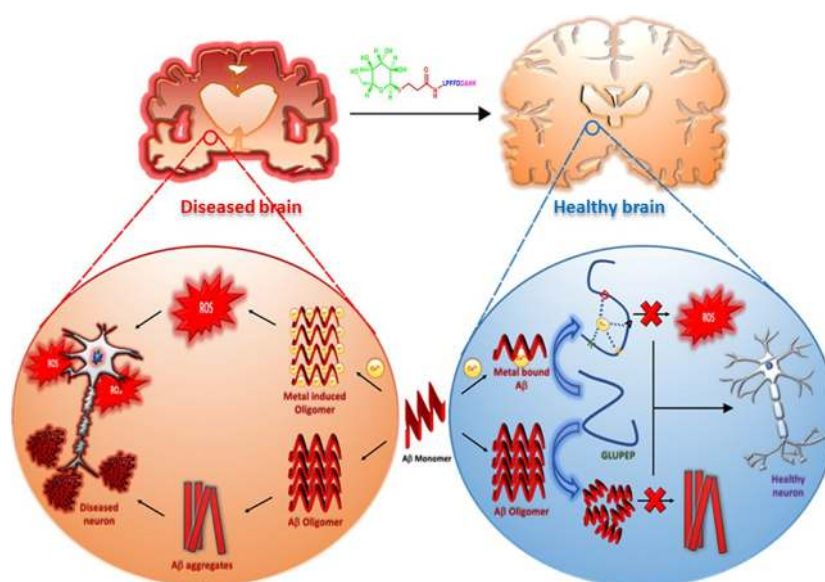


Figure 9. Mechanism for inhibition of metal-mediated and metal-independent amyloid toxicity.

were purchased from Spectrochem. Dichloromethane (DCM), *N,N'*-dimethylformamide (DMF), 4-dimethylaminopyridine (DMAP), hydrazine hydrate, methanol, ethyl acetate, 3-coumarin carboxylic acid (3-CCA), thioflavin-T, trifluoroacetic acid, hydrogen peroxide (30% solution), diethyl ether, acetic anhydride, deferoxamine, and 2,7-dichlorofluorescein diacetate (DCFDA) were purchased from Merck (Germany). 3-Mercaptopropionic acid and boron trifluoride etherate were purchased from TCI Pvt. Ltd. β -D-Glucose was obtained from Qualligens. Copper chloride was bought from SRL Pvt., Ltd. 3-(4,5-Dimethylthiazol-2-yl)-2,5-diphenyltetrazolium bromide (MTT) and dimethylsulfoxide (DMSO) for cell culture were purchased from Sigma-Aldrich. All the different sera and culture media were bought from Invitrogen. HPLC-grade water and acetonitrile were procured from J. T. Baker. β -Amyloid (1–42) was acquired from Alexotec (Sweden). Nitrocellulose membranes were obtained from Merck Millipore. Primary antibodies 6E10, A11, and OC were obtained from Bio Legend, Thermo Scientific, and Millipore, respectively. The BD Mitoscreen (mitochondrial membrane potential detection) JC-1 kit was bought from BD Biosciences. RP-HPLC (Shimadzu) with Symmetry C-18 (Waters) was used for purification of the glycopeptide and peptides. All compounds were used without further purification.

4.2. Synthesis and Purification of Peptides and Glycopeptides. The solid-phase peptide synthesis (SPPS) procedure was followed for synthesizing the peptides (DAHK, LPFFD, and LPFFDDAHK) using Rink amide AM resin. Fmoc-protected forms of the resin and amino acids were utilized to synthesize the peptides. Fmoc groups were deprotected using a solution of 20% piperidine in DMF. Resin-bound peptides were cleaved using a cleaving cocktail solution of TFA (91%), EDT (3%), MilliQ water (3%), and phenol (3%). The peptides were then precipitated dropwise in the precooled diethyl ether and stored at $-20\text{ }^{\circ}\text{C}$. Diethyl ether containing the crude peptide was centrifuged and purified by RP-HPLC (Figures S2A, S3A, and S4A), and the purified samples were characterized by ESI or MALDI mass spectroscopy (Figures S2B, S3B, and S4B).

To synthesize the glycopeptide (GluPeP), a convergent approach was followed (Scheme S1), where the peptide component (LPFFDDAHK) and glycocomponent (3-(2,3,4,6-tetraacetyl- α -D-glucopyranosyl)thiopropionic acid) were pre-synthesized. After the last deprotection step, the glycocomponent was coupled to the N-terminal of the resin-bound peptide. Acetylated glucose was deprotected using a solution of hydrazine hydrate in water (1:9). The glyco-coupled peptide was cleaved using a similar procedure as described earlier. Further purification was done by RP-HPLC (Figure S1A), and the purified samples were characterized by ESI mass spectrometry (Figure S1B).

4.3. Preparation of the $A\beta_{42}$ Fibril and Oligomer Sample. The $A\beta_{42}$ peptide was dissolved in hexafluoroisopropanol (HFIP) and kept for 1 h to dissociate the preformed aggregates.⁶⁵ HFIP was evaporated under a gentle nitrogen flow to get a white precipitate, which was then dried under vacuum and stored at $-20\text{ }^{\circ}\text{C}$ for further use. To prepare stock solution, $A\beta_{42}$ was dissolved first in the least possible amount of DMSO, and then the required concentration was achieved by making up the volume with PBS buffer (pH = 7.4, 10 mM).

To obtain the fibril aggregates, a desired amount of $A\beta_{42}$ in PBS (pH = 7.4, 10 mM) was kept in constant agitation at $37\text{ }^{\circ}\text{C}$ for 24 h.⁶⁶ To validate the formation of fibrils, ThT and dot blot assays were performed. Then, to prepare the oligomeric samples, $A\beta_{42}$ peptide solution in PBS was incubated at $37\text{ }^{\circ}\text{C}$ for 1 h and then was transferred to be incubated at $4\text{ }^{\circ}\text{C}$ for the next 24 h. Then, the solution was centrifuged at 15,000g, and the supernatant of the solution was used in the experiments.⁴⁶ The formation of $A\beta_{42}$ oligomers was confirmed using similar dot blot and ThT assays.

4.4. Preparation of the Cu^{2+} -Mediated $A\beta_{42}$ Aggregate Sample. Cu^{2+} -mediated $A\beta_{42}$ aggregate samples were prepared using a substoichiometric amount of Cu^{2+} . $A\beta_{42}$ and Cu^{2+} were mixed in a 1:0.4 ratio in PBS (10 mM, pH = 7.4) to prepare a final solution with a volume of $50\text{ }\mu\text{L}$. The solution was kept for incubation at $37\text{ }^{\circ}\text{C}$ at 150 rpm of constant shaking for 72 h. The formation of aggregates was confirmed by the ThT assay.

4.5. Determining the Inhibition of A β 42 Aggregates Using the ThT Fluorescence Assay. A β 42 (10 mM) was co-incubated with 10 μ M of all the compounds (i.e., glucose, DAHK, LPFFD, and Glupez) to form fibrils and oligomers according to the mentioned procedure. For the control experiment, only PBS was used. A 100 μ M stock solution of ThT in PBS was prepared from which a final concentration of 10 μ M was used to quantify the A β 42 fibrillar and oligomeric aggregates remaining intact. The fluorescence intensity was determined using a Quanta Master spectrofluorometer (QM-40) at an excitation wavelength of 435 nm and an emission wavelength of 485 nm (slit width = 1.25 nm).^{63,64} The fluorescence intensity of the blank solution was subtracted from each fluorescence measurement. The fluorescence intensity of only the A β 42 solution was fixed as 100%, and all the data were measured accordingly. The whole procedure was repeated again with different concentrations of Glupez (2.5–20 μ M) and also repeated to detect the inhibition of Cu²⁺-mediated aggregation. All the experiments were repeated three times, and a *t* test was performed to analyze the data.

4.6. Dot Blot Analysis. Different amounts of Glupez (5, 10, and 20 μ M) were mixed individually with A β 42 (10 μ M) in two separate sets of solutions. One set was subjected to incubation with constant shaking at 37 °C for 48 h to form fibrils. The other one was incubated at 37 °C for 1 h and then kept at 4 °C for 24 h to form oligomers. Then, the incubated solutions were centrifuged at 15,000g for 15 min and the supernatant was spotted on a nitrocellulose membrane. To block the nonspecific sites, the paper was soaked in 5% bovine serum albumin (BSA) in TBST buffer for 1 h at 37 °C. The nitrocellulose papers were reacted individually with the primary antibodies 6E10 (detects all forms of A β 42, 1:3000), A11 (detects specifically oligomers, 1:3000), and OC (detects fibrils only, 1:3000) overnight at 4 °C. The membranes were then washed three times, each with TBST buffer for 5 min. They were then kept for incubation along with horseradish peroxidase (HRP)-conjugated anti-mouse and anti-rabbit secondary antibodies (1:10000) for a minimum of 1 h at 37 °C. All the membranes were again washed with TBST buffer three times for 5 min. Lastly, the membranes were reacted with an enhanced chemiluminescence agent for 2 min. Biorad ChemiDoc Touch was used to record the chemiluminescence intensity. The relative decrement in aggregation was determined by comparing the chemiluminescence intensity to that of the control (only A β).⁶⁷

4.7. Molecular Docking Study. AutoDock Vina version 1.1.2⁶⁸ was used to carry out docking studies. All the ligand structures (i.e., Glupez, LPFFD, DAHK, glucose) were energy-minimized in Avogadro software using the MMFF94 force field. The protein structures of the A β 42 monomer (PDB ID: 1IYT) and fibril (PDB ID: 5KK3) were redeemed from the RCSB Protein Data Bank.⁵³ Blind docking studies were performed to recognize the binding sites of the highest probability. PyMOL (The PyMOL Molecular Graphics System, version 1.7.4 Schrödinger, LLC) was used to analyze results and record poses.

4.8. ·OH Radical Generation Measurement by the Ascorbate Assay. Solutions of 3-CCA (50 μ M) and Cu²⁺ (5 μ M) were prepared in PBS (10 mM, pH = 7.4), and each peptide (DAHK, LPFFD), glucose, and the glycopeptide Glupez were added independently to this solution to have a final concentration of 10 μ M. Next, deferoxamine with a final concentration of 1 μ M was added to this solution. Deferox-

amine was added to inhibit the iron (Fe²⁺ and Fe³⁺ that are present in PBS) from taking part in the redox cycle. Lastly, an excess amount of reductant sodium ascorbate (150 μ M) was added, and the solution was incubated for the next 70 min. Generated hydroxyl radicals converted nonfluorescent 3-CCA to fluorescent 7-OH-CCA (λ_{ex} = 395 nm and λ_{em} = 452 nm).³⁴ A Quanta Master spectrofluorometer (QM-40) was used to detect the fluorescence intensity at 452 nm as a function of ROS generation.

4.9. Tyrosine Fluorescence Spectroscopy. The intrinsic fluorescence of TYR10 (excitation: 285 nm and emission: 308 nm) of the A β 42 peptide gets diminished upon binding with Cu²⁺.⁵⁵ Treating the A β 42–Cu²⁺ complex with the chelating agent Glupez is expected to extract Cu²⁺ out and restore the fluorescence intensity. Therefore, the fluorescence intensity at 308 nm was measured to understand the extent of Cu²⁺ removal from the A β 42–Cu²⁺ complex by Glupez. For this, a solution of A β 42 (10 μ M) was prepared in PBS buffer (10 mM, pH = 7.4), and fluorescence was measured at 308 nm (positive control). Next, Cu²⁺ was added to the same solution to make a concentration of 10 μ M. After incubating for the next 30 min at 37 °C, fluorescence was again recorded to have a large decrement in fluorescence (negative control). Finally, Glupez (10 μ M) was added to the solution, and once again, fluorescence was measured.

4.10. Serum Stability Assay. Lipid components of the serum were precipitated by centrifuging it at 15,000g for 20 min. Solutions (100 μ M) of the peptides (DAHK, LPFFD, LPFFDDAHK) and Glupez were incubated with the supernatant for the next 24 h. At every 0, 4, 6, 12, and 24 h, triplicate solutions of 100 μ L were taken, and 100 μ L of acetonitrile was added to precipitate out serum proteins. To inhibit the serum protease activity, these solutions were kept at 4 °C for 30 min. Then, the solutions were centrifuged again, and the supernatant was analyzed using RP-HPLC (flow rate: 0.7 mL/min) to detect the remaining peptides and glycopeptides.⁶⁹ Lastly, the change in the intensity profile of the compounds with time was plotted.

4.11. In Vitro Evaluation of A β 42–Cu²⁺-Mediated Toxicity. This experiment was performed by seeding PC12 cells in a 96-well plate at 37 °C in a 5% CO₂ environment for 24 h. After 24 h, the media were replaced with media having a low serum concentration (2% serum concentration). Then, the cells were incubated with A β 42–Cu²⁺ (10 μ M) in the individual presence of peptides (10 μ M of DAHK and LPFFD), glucose (10 μ M), and Glupez (10 and 20 μ M) with a large amount of ascorbate (100 μ M). MTT (3-(4,5-dimethylthiazol-2-yl)-2,5-diphenyltetrazolium bromide) (10 mg/mL) was added to each well and incubated at 37 °C for 4 h. Cellular reductase enzymes of viable cells reduce MTT into purple-colored formazan. After 4 h, the media were discarded, and the formazan was dissolved with DMSO/MeOH (1:1 v/v). The absorption intensity of formazan was determined as a function of viable cells at 570 nm using a microplate ELISA reader.⁷⁰ The percentage of cell viability was determined by using the following equation on the absorption data.

$$\% \text{cell viability} = \left[\frac{\text{abs}_{570}(\text{treated cells}) - \text{abs}_{570}(\text{blank})}{\text{abs}_{570}(\text{untreated cells}) - \text{abs}_{570}(\text{blank})} \right] \times 100$$

4.12. Performing the JC-1 Assay to Assess the MMP.

Initially, we plated PC12 cells in six-well plates and cultured them overnight. Next, the cells were treated with 100 ng/mL NGF in differentiation medium and differentiated into neurons in 5 days. After this, the PC12-derived neurons were treated with $A\beta_{42}-Cu^{2+}$ (10 μ M) and $A\beta_{42}-Cu^{2+}$ (10 μ M) along with Glupez (10 μ M and 20 μ M) for 24 h. Next, the cells were dislodged, and the intracellular mitochondrial membrane potential ($\Delta\psi_m$) was measured with the aid of BD MitoScreen following the manufacturer's instructions. In brief, first, the dislodged cells were treated with a working concentration of JC-1 (5,5',6,6'-tetrachloro-1,1',3,3'-tetraethylbenzimidazolcarbocyanine iodide) dye diluted in 1 \times assay buffer, which is prepared from a 10 \times assay buffer. JC-1 is a membrane-permeable dye that can penetrate into cells and induce fluorescence, reflecting the status of the membrane polarization ($\Delta\psi$). The cells were incubated with the dye for 25 min at 37 $^{\circ}$ C in a CO₂ incubator. After that, the cells were washed with the assay buffer, and the membrane potential was determined through FACS (LSRFORTESA) at 527 and 590 nm.

4.13. Measuring the Intracellular ROS Level by the DCFDA Assay. To explore the effect of Glupez on $A\beta_{42}-Cu^{2+}$ -mediated intracellular oxidative stress, the DCFDA assay was performed. PC12 cells were seeded on a 96-well plate at 37 $^{\circ}$ C in a 5% CO₂ environment. After incubation for 20 h, when the cells were properly grown, the media were changed and kept for another incubation period of 4 h. Next, the cells were washed with PBS and incubated with 2,7-dichlorodihydrofluoresceindiacetate (DCFDA, λ_{ex} = 495 nm, λ_{em} = 529 nm) for another half an hour. Cells were washed again and incubated with $A\beta_{42}-Cu^{2+}$ (10 μ M) and ascorbate (300 μ M) as a control solution. The control solution was incubated alone and separately with peptides (10 μ M LPPFD and DAHK), glucose (10 μ M), and Glupez (5, 10, and 20 μ M) at 37 $^{\circ}$ C for 40 min. Cells were washed, and the fluorescence intensity at 529 nm was measured using a microplate reader. The significance of the result was determined by performing two-tailed Student's *t* test.

4.14. Blood–Brain Barrier Permeability Assay. Mice were divided into two groups, each containing three mice. A solution of Glupez (2.5 mM) was made in saline. Then, 100 μ L of the saline solution was injected intraperitoneally into the first group, keeping a dosage value of 10 mL/kg body weight. The second group was treated in the same way as nonglycosylated LPPFD/DAHK. After 6 h, mice were anesthetized properly before subjecting to sacrifice. Blood was drained out totally from the body through transcardial perfusion. After collecting the brain in PBS, the meninges and blood vessels were carefully removed. The cortex was dissected out from the brain to prepare a homogenate in acetonitrile–water solution (1:1). It was then centrifuged at 10,000g for 10 min to separate out the brain vasculature, red blood cells, and brain nuclei.⁷¹ The supernatant was then detected through mass spectroscopy for the presence molecular peaks of Glupez and LPPFD/DAHK.

4.15. Data Analysis. Images of the dot blot study were analyzed using Image J software. To measure spectroscopic data and histograms, Origin 8.5 pro software was used. Statistical calculations were done by performing ANOVA and two-tailed Student's *t* test. Statistical values of **P* \leq 0.05 and ***P* \leq 0.03 were allocated for different experiments accordingly.

■ ASSOCIATED CONTENT

SI Supporting Information

The Supporting Information is available free of charge at <https://pubs.acs.org/doi/10.1021/acsomega.0c01028>.

Scheme of Glupez, synthetic procedure, HPLC chromatogram and mass spectrum, densitometric plots of dot blot assays, ThT fluorometric assay in the presence of copper, several molecular interaction studies, UV–vis spectra, MTT assay, quantitative image analysis of the DCFDA microscopic study, quantitative bar diagram representation of JC1 data, and mass spectra of mice brain extract (PDF)

■ AUTHOR INFORMATION

Corresponding Author

Surajit Ghosh – *Organic and Medicinal Chemistry and Structural Biology and Bioinformatics Division, CSIR-Indian Institute of Chemical Biology, Kolkata 700 032, WB, India; Department of Bioscience & Bioengineering, Indian Institute of Technology Jodhpur, Karwar, Rajasthan 342037, India; Academy of Scientific and Innovative Research (AcSIR), Ghaziabad 201002, India; orcid.org/0000-0002-8203-8613; Phone: +91-33-2499-5872; Email: sghosh@iitj.ac.in; Fax: +91-33-2473-5197/0284*

Authors

Rajsekhar Roy – *Department of Bioscience & Bioengineering, Indian Institute of Technology Jodhpur, Karwar, Rajasthan 342037, India*

Krishnangsu Pradhan – *Organic and Medicinal Chemistry and Structural Biology and Bioinformatics Division, CSIR-Indian Institute of Chemical Biology, Kolkata 700 032, WB, India*

Juhee Khan – *Organic and Medicinal Chemistry and Structural Biology and Bioinformatics Division, CSIR-Indian Institute of Chemical Biology, Kolkata 700 032, WB, India; orcid.org/0000-0002-9955-6505*

Gaurav Das – *Organic and Medicinal Chemistry and Structural Biology and Bioinformatics Division, CSIR-Indian Institute of Chemical Biology, Kolkata 700 032, WB, India; orcid.org/0000-0002-8432-5384*

Nabanita Mukherjee – *Department of Bioscience & Bioengineering, Indian Institute of Technology Jodhpur, Karwar, Rajasthan 342037, India*

Durba Das – *Department of Bioscience & Bioengineering, Indian Institute of Technology Jodhpur, Karwar, Rajasthan 342037, India*

Complete contact information is available at: <https://pubs.acs.org/doi/10.1021/acsomega.0c01028>

Author Contributions

R.R. carried out synthesis, purification, characterization of Glupez, major experiments, and analysis of results and helped S.G. in writing and formulating the manuscript. K.P. helped R.R. in biophysical assays and in synthesis. J. K. performed the MTT assay, DCFDA fluorometric assay, and BBB permeability. R.R. helped J.K. in determining the BBB permeability. G.D. performed the dot blot assay, DCFDA image analysis, and JC-1 assay. N.M. and D.D. helped R.R. in formulating the manuscript and a few experiments. S.G. conceived the idea, designed and monitored all the experiments, and wrote the manuscript.

Notes

The authors declare no competing financial interest.

ACKNOWLEDGMENTS

R.R. and N. M. thank IIT Jodhpur, K.P. thanks UGC, J.K. thanks DST, and G.D. thanks ICMR for awarding their fellowships. D. D. thanks Director IIT Jodhpur for academic support. S.G. kindly acknowledges SERB, India (CRG/2019/000670), for financial assistance. S.G. also thanks CSIR-IICB Kolkata and IIT Jodhpur for infrastructure.

ABBREVIATION

A β : amyloid beta; AD: Alzheimer's disease; DCFDA: 2',7'-dichlorofluorescein diacetate; MTT: 3-(4,5-dimethylthiazol-2-yl)-2,5-diphenyltetrazolium bromide; PDB: Protein Data Bank

REFERENCES

- (1) Wang, J.; Gu, B. J.; Masters, C. L.; Wang, Y.-J. A systemic view of Alzheimer disease—insights from amyloid- β metabolism beyond the brain. *Nat Rev Neurol* **2017**, *13*, 612.
- (2) Holtzman, D. M.; Morris, J. C.; Goate, A. M. Alzheimer's Disease: The Challenge of the Second Century. *Sci. Transl. Med.* **2011**, *3*, 77.
- (3) Rajasekhar, K.; Chakrabarti, M.; Govindaraju, T. Function and toxicity of amyloid beta and recent therapeutic interventions targeting amyloid beta in Alzheimer's disease. *Chem. Commun.* **2015**, *51*, 13434–13450.
- (4) Rajasekhar, K.; Govindaraju, T. Current progress, challenges and future prospects of diagnostic and therapeutic interventions in Alzheimer's disease. *RSC Adv.* **2018**, *8*, 23780–23804.
- (5) Davies, P.; Maloney, A. J. F. Selective loss of central cholinergic neurons in Alzheimer's disease. *The Lancet* **1976**, *308*, 1403.
- (6) Selkoe, D. J. The molecular pathology of Alzheimer's disease. *Neuron* **1991**, *6*, 487–498.
- (7) Bush, A. I.; Pettingell, W. H.; Multhaup, G.; Paradis, M. D.; Vonsattel, J. P.; Gusella, J. F.; Beyreuther, K.; Masters, C. L.; Tanzi, R. E. Rapid induction of Alzheimer A beta amyloid formation by zinc. *Science* **1994**, *265*, 1464–1467.
- (8) Frost, B.; Jacks, R. L.; Diamond, M. I. Propagation of tau misfolding from the outside to the inside of a cell. *J. Biol. Chem.* **2009**, *284*, 12845–12852.
- (9) Butterfield, D. A.; Halliwell, B. Oxidative stress, dysfunctional glucose metabolism and Alzheimer disease. *Nat Rev Neurosci* **2019**, *20*, 148–160.
- (10) Härd, T.; Lendel, C. Inhibition of amyloid formation. *J. Mol. Biol.* **2012**, *421*, 441–465.
- (11) Jha, N. N.; Kumar, R.; Panigrahi, R.; Navalkar, A.; Ghosh, D.; Sahay, S.; Mondal, M.; Kumar, A.; Maji, S. K. Comparison of α -Synuclein Fibril Inhibition by Four Different Amyloid Inhibitors. *ACS Chem. Neurosci.* **2017**, *8*, 2722–2733.
- (12) Walsh, D. M.; Selkoe, D. J. A β oligomers—a decade of discovery. *J. Neurochem.* **2007**, *101*, 1172–1184.
- (13) Tjernberg, L. O.; Näslund, J.; Lindqvist, F.; Johansson, J.; Karlström, A. R.; Thyberg, J.; Terenius, L.; Nordstedt, C. Arrest of amyloid fibril formation by a pentapeptide ligand. *J. Biol. Chem.* **1996**, *271*, 8545–8548.
- (14) Rajasekhar, K.; Suresh, S. N.; Manjithaya, R.; Govindaraju, T. Rationally designed peptidomimetic modulators of A β toxicity in Alzheimer's disease. *Sci. Rep.* **2015**, *5*, 8139.
- (15) Lowe, T. L.; Strzelec, A.; Kiessling, L. L.; Murphy, R. M. Structure–function relationships for inhibitors of β -amyloid toxicity containing the recognition sequence KLVFF. *Biochemistry* **2001**, *40*, 7882–7889.
- (16) Soto, C.; Sigurdsson, E. M.; Morelli, L.; Kumar, R. A.; Castaño, E. M.; Frangione, B. β -sheet breaker peptides inhibit fibrillogenesis in a rat brain model of amyloidosis: implications for Alzheimer's therapy. *Nat. Med.* **1998**, *4*, 822.
- (17) Pfaender, S.; Grabrucker, A. M. Characterization of biometal profiles in neurological disorders. *Metallomics* **2014**, *6*, 960–977.
- (18) Braidy, N.; Poljak, A.; Marjo, C.; Rutledge, H.; Rich, A.; Jugder, B. E.; Jayasena, T.; Inestrosa, N. C.; Sachdev, P. S. Identification of cerebral metal ion imbalance in the brain of aging Octodon degus. *Front Aging Neurosci* **2017**, *9*, 66.
- (19) Maynard, C. J.; Bush, A. I.; Masters, C. L.; Cappai, R.; Li, Q.-X. Metals and amyloid- β in Alzheimer's disease. *Int. J. Clin. Exp. Pathol.* **2005**, *86*, 147–159.
- (20) Hensley, K.; Carney, J. M.; Mattson, M. P.; Aksenova, M.; Harris, M.; Wu, J. F.; Floyd, R. A.; Butterfield, D. A. A model for beta-amyloid aggregation and neurotoxicity based on free radical generation by the peptide: relevance to Alzheimer disease. *Proc. Natl. Acad. Sci. U. S. A.* **1994**, *91*, 3270–3274.
- (21) Dikalov, S. I.; Vitek, M. P.; Maples, K. R.; Mason, R. P. Amyloid β peptides do not form peptide-derived free radicals spontaneously, but can enhance metal-catalyzed oxidation of hydroxylamines to nitroxides. *J. Biol. Chem.* **1999**, *274*, 9392–9399.
- (22) Huang, X.; Atwood, C. S.; Hartshorn, M. A.; Multhaup, G.; Goldstein, L. E.; Scarpa, R. C.; Cuajungco, M. P.; Gray, D. N.; Lim, J.; Moir, R. D.; Tanzi, R. E. The A β peptide of Alzheimer's disease directly produces hydrogen peroxide through metal ion reduction. *Biochemistry* **1999**, *38*, 7609–7616.
- (23) Varadarajan, S.; Kanski, J.; Aksenova, M.; Lauderback, C.; Butterfield, D. A. Different Mechanisms of Oxidative Stress and Neurotoxicity for Alzheimer's A β (1–42) and A β (25–35). *J. Am. Chem. Soc.* **2001**, *123*, 5625–5631.
- (24) Bélanger, M.; Allaman, I.; Magistretti, P. J. Brain energy metabolism: focus on astrocyte-neuron metabolic cooperation. *Cell Metab.* **2011**, *14*, 724–738.
- (25) Jiang, D.; Men, L.; Wang, J.; Zhang, Y.; Chickenyen, S.; Wang, Y.; Zhou, F. Redox reactions of copper complexes formed with different β -amyloid peptides and their neuropathological relevance. *Biochemistry* **2007**, *46*, 9270–9282.
- (26) Eskici, G.; Axelsen, P. H. Copper and oxidative stress in the pathogenesis of Alzheimer's disease. *Biochemistry* **2012**, *51*, 6289–6311.
- (27) Adlard, P. A.; Cherny, R. A.; Finkelstein, D. I.; Gautier, E.; Robb, E.; Cortes, M.; Volitakis, I.; Liu, X.; Smith, J. P.; Perez, K.; Laughton, K. Rapid restoration of cognition in Alzheimer's transgenic mice with 8-hydroxy quinoline analogs is associated with decreased interstitial A β . *Neuron* **2008**, *59*, 43–55.
- (28) Geng, J.; Li, M.; Wu, L.; Chen, C.; Qu, X. Mesoporous silica nanoparticle-based H₂O₂ responsive controlled-release system used for Alzheimer's disease treatment. *Adv. Healthcare Mater.* **2012**, *1*, 332–336.
- (29) Jensen, M.; Canning, A.; Chiha, S.; Bouquerel, P.; Pedersen, J. T.; Østergaard, J.; Cuvillier, O.; Sasaki, I.; Hureau, C.; Faller, P. Inhibition of Cu-amyloid- β by using bifunctional peptides with β -sheet breaker and chelator moieties. *Chem. – Eur. J.* **2012**, *18*, 4836–4839.
- (30) Zhang, Q.; Hu, X.; Wang, W.; Yuan, Z. Study of a bifunctional A β aggregation inhibitor with the abilities of anti-amyloid- β and copper chelation. *Biomacromolecules* **2016**, *17*, 661–668.
- (31) Rajasekhar, K.; Madhu, C.; Govindaraju, T. Natural tripeptide-based inhibitor of multifaceted amyloid β toxicity. *ACS Chem. Neurosci.* **2016**, *7*, 1300–1310.
- (32) Harford, C.; Sarkar, B. Amino terminal Cu (II)- and Ni (II)-binding (ATCUN) motif of proteins and peptides: metal binding, DNA cleavage, and other properties. *Acc. Chem. Res.* **1997**, *30*, 123–130.
- (33) Neupane, K. P.; Aldous, A. R.; Kritzer, J. A. Metal-binding and redox properties of substituted linear and cyclic ATCUN motifs. *J. Inorg. Biochem.* **2014**, *139*, 65–76.
- (34) Guilloureau, L.; Combalbert, S.; Sourmia-Saquet, A.; Mazarguil, H.; Faller, P. Redox Chemistry of Copper–Amyloid- β : The Generation of Hydroxyl Radical in the Presence of Ascorbate is Linked to Redox-Potentials and Aggregation State. *ChemBioChem* **2007**, *8*, 1317–1325.

- (35) Buccella, D.; Lim, M. H.; Morrow, J. R. Metals in Biology: From Metallomics to Trafficking. *Inorg. Chem.* **2019**, *58*, 13505–13508.
- (36) Tsitovich, P. B.; Cox, J. M.; Benedict, J. B.; Morrow, J. R. Six-coordinate iron (II) and cobalt (II) paraSHIFT agents for measuring temperature by magnetic resonance spectroscopy. *Inorg. Chem.* **2016**, *55*, 700–716.
- (37) Costa, M.; Ortiz, A. M.; Pérez, A.; Mestre, A.; Ruiz, A.; Boada, M.; Grancha, S. Increased Albumin Oxidation in Cerebrospinal Fluid and Plasma from Alzheimer's Disease Patients. *J. Alzheimers Dis.* **2018**, *63*, 1–1404.
- (38) Böttger, R.; Hoffmann, R.; Knappe, D. Differential stability of therapeutic peptides with different proteolytic cleavage sites in blood, plasma and serum. *PLoS One* **2017**, *12*, No. e0178943.
- (39) Qyit, N.; Rubin, S. J. S.; Urban, T. J. ; Mochly-Rosen, D.; Gross, E. R. Peptidomimetic therapeutics: scientific approaches and opportunities. *Drug Discovery Today* **2017**, *22*, 454–462.
- (40) Moradi, S. V.; Hussein, W. M.; Varamini, P.; Simerska, P.; Toth, I. Glycosylation, an effective synthetic strategy to improve the bioavailability of therapeutic peptides. *Chem. Sci.* **2016**, *7*, 2492–2500.
- (41) Sinopoli, A.; Giuffrida, A.; Tomasello, M. F.; Giuffrida, M. L.; Leone, M.; Attanasio, F.; Caraci, F.; De Bona, P.; Naletova, I.; Saviano, M.; Copani, A. Ac-LPFDD-Th: A Trehalose-Conjugated Peptidomimetic as a Strong Suppressor of Amyloid- β Oligomer Formation and Cytotoxicity. *ChemBioChem* **2016**, *17*, 1541–1549.
- (42) Ryan, P.; Patel, B.; Makwana, V.; Jadhav, H. R.; Kiefel, M.; Davey, A.; Reekie, T. A.; Rudrawar, S.; Kassioch, M. Peptides, peptidomimetics, and carbohydrate-peptide conjugates as amyloidogenic aggregation inhibitors for Alzheimer's disease. *ACS Chem. Neurosci.* **2018**, *9*, 1530–1551.
- (43) Rana, M.; Sharma, A. K. Cu and Zn interactions with A β peptides: Consequence of coordination on aggregation and formation of neurotoxic soluble A β oligomers. *Metallomics* **2019**, *11*, 64–84.
- (44) Andreotti, A. H.; Kahne, D. The effects of glycosylation on peptide backbone conformation. *J. Am. Chem. Soc.* **1993**, *115*, 3352–3353.
- (45) Naiki, H.; Higuchi, K.; Hosokawa, M.; Takeda, T. Fluorometric determination of amyloid fibrils *in vitro* using the fluorescent dye, thioflavine T. *Anal. Biochem.* **1989**, *177*, 244–249.
- (46) Ryan, D. A.; Narrow, W. C.; Federoff, H. J.; Bowers, W. J. An improved method for generating consistent soluble amyloid beta oligomer preparations for *in vitro* neurotoxicity studies. *J. Neurosci. Methods* **2010**, *190*, 171–179.
- (47) Colletier, J.-P.; Laganowsky, A.; Landau, M.; Zhao, M.; Soriaga, A. B.; Goldschmidt, L.; Flot, D.; Cascio, D.; Sawaya, M. R.; Eisenberg, D. Molecular basis for amyloid- β polymorphism. *Proc. Natl. Acad. Sci. U. S. A.* **2011**, *108*, 16938–16943.
- (48) Sakono, M.; Zako, T. Amyloid oligomers: formation and toxicity of A β oligomers. *FEBS J.* **2010**, *277*, 1348–1358.
- (49) Bhasikuttan, A. C.; Mohanty, J. Detection, inhibition and disintegration of amyloid fibrils: the role of optical probes and macrocyclic receptors. *Chem. Commun.* **2017**, *53*, 2789–2809.
- (50) Turner, J. P.; Lutz-Rechtin, T.; Moore, K. A.; Rogers, L.; Bhawe, O.; Moss, M. A.; Servoss, S. L. Rationally designed peptoids modulate aggregation of amyloid-beta 40. *ACS Chem. Neurosci.* **2014**, *5*, 552–558.
- (51) Faller, P.; Hureau, C.; Penna, G. L. Metal ions and intrinsically disordered proteins and peptides: from Cu/Zn amyloid- β to general principles. *Acc. Chem. Res.* **2014**, *47*, 2252–2259.
- (52) Crescenzi, O.; Tomaselli, S.; Guerrini, R.; Salvadori, S.; D'Ursi, A. M.; Temussi, P. A.; Picone, D. Solution structure of the Alzheimer's disease amyloid beta-peptide (1–42). *Eur. J. Biochem.* **2002**, *269*, 5642–5648.
- (53) Colvin, M. T.; Silvers, R.; Ni, Q. Z.; Can, T. V.; Sergeyev, I.; Rosay, M.; Donovan, K. J.; Michael, B.; Wall, J.; Linse, S.; Griffin, R. G. Atomic resolution structure of monomorphic A β 42 amyloid fibrils. *J. Am. Chem. Soc.* **2016**, *138*, 9663–9674.
- (54) Arrigoni, F.; Prosdoci, T.; Mollica, L.; De Gioia, L.; Zampella, G.; Bertini, L. Copper reduction and dioxygen activation in Cu-amyloid beta peptide complexes: insight from molecular modelling. *Metallomics* **2018**, *10*, 1618–1630.
- (55) Muthuraj, B.; Layek, S.; Balaji, S. N.; Trivedi, V.; Iyer, P. K. Multiple function fluorescein probe performs metal chelation, disaggregation, and modulation of aggregated A β and A β -Cu complex. *ACS Chem. Neurosci.* **2015**, *6*, 1880–1891.
- (56) Chen, W. T.; Liao, Y. H.; Yu, H. M.; Cheng, I. H.; Chen, Y. R. Distinct effects of Zn²⁺, Cu²⁺, Fe³⁺, and Al³⁺ on amyloid- β stability, oligomerization, and aggregation amyloid- β destabilization promotes annular protofibril formation. *J. Biol. Chem.* **2011**, *286*, 9646–9656.
- (57) Williams, T. L.; Day, I. J.; Serpell, L. C. The effect of Alzheimer's A β aggregation state on the permeation of biomimetic lipid vesicles. *Langmuir* **2010**, *26*, 17260–17268.
- (58) Stockert, J. C.; Horobin, R. W.; Colombo, L. L.; Blázquez-Castro, A. Tetrazolium salts and formazan products in Cell Biology: Viability assessment, fluorescence imaging, and labeling perspectives. *Acta Histochem.* **2018**, *120*, 159–167.
- (59) Yu, S. L.; Lin, S. B.; Yu, Y. L.; Chien, M. H.; Su, K. J.; Lin, C. J.; Yiang, G. T.; Lin, C. C.; Chan, D. C.; Harn, H. J.; Chen, Y. L. S. Isochaulactone protects PC12 cell against H₂O₂ induced oxidative stress and exerts the potent anti-aging effects in D-galactose aging mouse model. *Acta Pharmacol. Sin.* **2010**, *31*, 1532–1540.
- (60) Fosgerau, K.; Hoffmann, T. Peptide therapeutics: Current status and future directions. *Drug Discovery Today* **2015**, *20*, 122–128.
- (61) Egleton, R. D.; Davis, T. P. Development of neuropeptide drugs that cross the blood-brain barrier. *NeuroRx* **2005**, *2*, 44–53.
- (62) Uchida, E.; Morimoto, K.; Kawasaki, N.; Ahmed, Y.; Said, A.; Hayakawa, T. Effect of active oxygen radicals on protein and carbohydrate moieties of recombinant human erythropoietin. *Free Radical Res.* **1997**, *27*, 311–323.
- (63) Pradhan, K.; Das, G.; Gupta, V.; Mondal, P.; Barman, S.; Khan, J.; Ghosh, S. Discovery of Neuroregenerative Peptoid from Amphibian Neuropeptide That Inhibits Amyloid- β Toxicity and Crosses Blood-Brain Barrier. *ACS Chem. Neurosci.* **2018**, *10*, 1355–1368.
- (64) Mondal, P.; Gupta, V.; Das, G.; Pradhan, K.; Khan, J.; Gharai, P. K.; Ghosh, S. Peptide-Based Acetylcholinesterase Inhibitor Crosses the Blood-Brain Barrier and Promotes Neuroprotection. *ACS Chem. Neurosci.* **2018**, *9*, 2838–2848.
- (65) Zhang-Haagen, B.; Biehl, R.; Nagel-Steger, L.; Radulescu, A.; Richter, D.; Willbold, D. Monomeric amyloid beta peptide in hexafluoroisopropanol detected by small angle neutron scattering. *PLoS One* **2016**, *11*, No. e0150267.
- (66) Jan, A.; Hartley, D. M.; Lashuel, H. A. Preparation and characterization of toxic A β aggregates for structural and functional studies in Alzheimer's disease research. *Nat. Protoc.* **2010**, *5*, 1186–1209.
- (67) Szaruga, M.; Munteanu, B.; Lismont, S.; Veugelen, S.; Horr , K.; Mercken, M.; Saido, T. C.; Ryan, N. S.; De Vos, T.; Savvides, S. N.; Gallardo, R.; Schymkowitz, J.; Rousseau, F.; Fox, N. C.; Hopf, C.; Strooper, B. D.; Ch avez-Guti rrez, L. Alzheimer's-causing mutations shift A β length by destabilizing γ -secretase-A β n interactions. *Cell* **2017**, *170*, 443–456.e14.
- (68) Trott, O.; Olson, A. J. AutoDock Vina: Improving the Speed and Accuracy of Docking with a New Scoring Function, Efficient Optimization, and Multithreading. *J. Comput. Chem.* **2010**, *31*, 455–461.
- (69) Kaniusaitė, M.; Tailhades, J.; Marschall, E. A.; Goode, R. J.; Schittenhelm, R. B.; Cryle, M. J. A proof-reading mechanism for non-proteinogenic amino acid incorporation into glycopeptide antibiotics. *Chem. Sci.* **2019**, *10*, 9466–9482.
- (70) Mekmouche, Y.; Coppel, Y.; Hochgr fe, K.; Guilloreau, L.; Talmard, C.; Mazarguil, H.; Faller, P. Characterization of the ZnII Binding to the Peptide Amyloid- β 1–16 linked to Alzheimer's Disease. *ChemBioChem* **2005**, *6*, 1663–1671.
- (71) Prades, R.; Oller-Salvia, B.; Schwarzmaier, M. S.; Selva, J.; Moros, M.; Balbi, M.; Gzazu, V.; de La Fuente, M. J.; Egea, G.; Plesnila, N.; Teixido, M.; Giralt, E. Applying the Retro-Enantio

Approach To Obtain a Peptide Capable of Overcoming the Blood-Brain Barrier. *Angew. Chem., Int. Ed.* **2015**, *54*, 3967–3972.